

# CCT2 enhances the proliferation and migration of head and neck squamous cell carcinoma via regulating cell cycle

**Lin Lu**

Hospital of Stomatology, Guanghua School of Stomatology, Sun Yat-Sen University

**Xuerong Li**

Hospital of Stomatology, Guanghua School of Stomatology, Sun Yat-Sen University

**Yiwei Zhao**

Hospital of Stomatology, Guanghua School of Stomatology, Sun Yat-Sen University

**Xuefan Zhai**

Hospital of Stomatology, Guanghua School of Stomatology, Sun Yat-Sen University

**Min Cai**

Hospital of Stomatology, Guanghua School of Stomatology, Sun Yat-Sen University

**Baicheng Bao**

Hospital of Stomatology, Guanghua School of Stomatology, Sun Yat-Sen University

**Menghuan Li**

Hospital of Stomatology, Guanghua School of Stomatology, Sun Yat-Sen University

**Jianbo Sun** (✉ [sunjb3@mail.sysu.edu.cn](mailto:sunjb3@mail.sysu.edu.cn))

Hospital of Stomatology, Guanghua School of Stomatology, Sun Yat-Sen University

---

## Research Article

**Keywords:** head and neck squamous cell carcinoma (HNSCC), CCT2, cyclin-CDK pathway, Cdc20, cell cycle

**Posted Date:** May 6th, 2022

**DOI:** <https://doi.org/10.21203/rs.3.rs-1612727/v1>

**License:** © ⓘ This work is licensed under a Creative Commons Attribution 4.0 International License.

[Read Full License](#)

---

# Abstract

Recent therapeutic advances have improved the survival of head and neck squamous cell carcinoma (HNSCC) patients, but the prognosis of HNSCC remains dismal. Further understanding of the underlying mechanism of HNSCC progression is still an urgent need. In this study, bioinformatics-based analysis revealed that Chaperonin containing TCP-1, subunit 2 (CCT2) is significantly upregulated in HNSCC and related to pathoclinical outcomes, which is validated by the fact that four human HNSCC cell lines all express higher CCT2 than the normal oral squamous cell line. Clinically, high CCT2 expression was positively associated with worse overall survival (OS) and TNM classification in HNSCC patients. Further study indicated that suppression of CCT2 by RNA interference significantly inhibits cell proliferation, migration and invasion, arrests cell cycle at G2 phase, and prevents epithelial-mesenchymal transition (EMT) of both SAS and HSC-3 cell lines. In vivo assays further verified that CCT2 knockdown inhibited tumor growth in HNSCC. Moreover, knockdown of CCT2 led to the significant decrease of Cdc20 as well as cyclin D1, cyclin E1, and CDK6 while increase of GSK3- $\alpha/\beta$  and p27, which shed light into molecular mechanism of CCT2 function. In conclusion, elevated CCT2 expression promotes HNSCC cell proliferation via Cdc20 mediated cyclin-CDK pathway and CCT2 would be a valuable prognostic biomarker and therapeutic target in HNSCC.

## Introduction

Head and neck squamous cell carcinoma (HNSCC) includes an anatomically heterogenous group of solid tumors that mainly originate in the epithelial cells of the oral cavity, pharynx(naso-, oro-, and hypopharynx) and larynx[1]. Most of HNSCC is oral squamous cell carcinoma (OSCC). With a yearly incidence of 655,000 cases worldwide, HNSCC is the 6th most common malignancies[2]. As HNSCC usually progresses without obvious symptoms, around 2/3 of patients present with advanced disease, often with regional lymph node involvement, while 10% present with distant metastases. The 5-years survival rate of HNSCC in all stages is about 60%, and can be even worse for specific primary sites such as hypopharynx[3]. Therefore, identifying early prognostic markers and potential drug targets is of great importance to improve prognosis and individualized treatments.

Chaperonin containing TCP-1 (CCT, also known as TRiC or c-cpn), a member of group II (eukaryotic) chaperonin family, consists of eight homologous subunits (CCT1, 2, 3, 4, 5, 6, 7, 8)[4]. The subunits are assembled in two back-to-back stacked oligomeric rings, forming a cage where protein folding and refolding take place in the presence of ATP[5–7]. CCT has been shown to interact with 5–10% of whole proteome that is correlated with cell growth[8], proliferation and apoptosis in normal and tumor cells including tumor suppressor Von Hippel-Lindau (VHL), p53, pro- oncogenic proteins signal transducer and activator of transcription 3 (STAT3), cell cycle regulatory proteins cell division cycle protein 20 (Cdc20), tubulins, cyclin B, cyclin E, and actins, many of which are implicated in oncogenesis[9–14]. Emerging evidences have implicated that CCT and its subunits play an important role in the development of many human malignancies such as breast cancer[15, 16], liver cancer[17–19], gastrointestinal cancer[20–22], lung cancer[23] and acute myeloid leukemia[24]. Moreover, the aberrant expression of certain members of

CCT family is found to have prognostic values in some malignancies. For example, overexpression of CCT3 and CCT8 is positively correlated with the histologic grades and tumor size of hepatocellular carcinoma, and predicts a poor prognosis[17, 18, 25]. In glioblastoma, higher expression and amplification of CCT6A associates negatively with survival rate[26]. And CCT2 is needed for tumor growth in colorectal[27], breast[15] and lung cancer[23].

CCT family proteins are highly expressed in HNSCC according to online public database, which needs validation with laboratorial experiments[28]. The function of CCT subunits in the carcinogenesis of HNSCC remains unclear. Hence, we studied the function of CCT2 in HNSCC and explored the underlying mechanisms.

## Results

### **CCT2 is upregulated in HNSCC and associated with worse pathoclinical outcomes**

We compared the mRNA expression level of CCT2 in HNSCC tissues and normal samples with GEPIA dataset (<http://gepia.cancer-pku.cn/>). The results showed that CCT2 expression level was higher in HNSCC tissues than in normal ones (Figure 1A) ( $|\text{Log}_2\text{FC}| > 1$  and  $q\text{value} < 0.01$ ). Moreover, The Kaplan-Meier curve and log-rank test analyses indicated that increased CCT2 was significantly associated with worse overall survival of patients with HNSCC but not with the disease free survival (Figure 1B). We next detected CCT2 expression in four HNSCC cell lines (SAS, HSC-3, CAL-27, HSC-6) and a normal oral squamous cell line(NOK) by western blot and qRT-PCR (Figure 1C&D). Compared with NOK cells, both mRNA and protein level of CCT2 were obviously upregulated in HNSCC cell lines.

To validate these data, obtained from public databases and our HNSCC line panel, in clinical human tumor samples, we detected CCT2 protein expression in 41 HNSCC tissues and their adjacent normal tissues via immunohistochemistry. The results indicated that CCT2 was significantly upregulated in HNSCC tissues with 80.48% positive rate (33/41), compared with the non-cancerous tissues (Figure 1E). Then we analyzed the clinical characteristics associated with CCT2 and found that high expression of CCT2 was significantly positively associated with American Joint Committee on Cancer (AJCC) clinical stage (AJCC 8th stage system)[29], TNM classification ( $p=0.014$ ), and maybe tumor size ( $p=0.059$ ), but not other clinical features (Table 1).

### **CCT2 promotes the proliferation, migration and invasion of HNSCC cells *in vitro***

To uncover the exact roles of CCT2 in tumorigenesis, we knocked down CCT2 in SAS and HSC-3 cells by shRNAs efficiently (Figure 2A-B & 3A-B). With the decrease of CCT2, the proliferation of the cancer cells was significantly inhibited as the CCK-8 curve (Figure 2C&3C) and EdU assay (Figure 2E&3E) showed. The results were further confirmed by colony formation assays, indicating a lower duplicating potential (Figure 2D&3D). Moreover, the wound healing assay showed significantly reduced migration ability in cancer cells expressing shCCT2 compared with the control (Figure 2F&3F). Further study indicated that the number of migrating cells in the CCT2-knockdown group was significantly lower than the control

group after cultured for 24h in Transwell apparatus or Boyden chambers coated with Matrigel (Figure 2G&3G). As epithelial-mesenchymal transition (EMT) is of great importance for tumor migration and invasion, we analyzed EMT-associated proteins by Western blot. The results showed that E-cadherin expression was markedly increased while N-cadherin and Slug expression were obviously decreased in CCT2 knockdown cells (Figure 2H&3H), suggesting that EMT was inhibited. All of these data indicated that CCT2 upregulation promoted the proliferation, migration and invasion of HNSCC cells.

### **Knockdown of CCT2 inhibits HNSCC growth *in vivo***

We then employed subcutaneous cell line-derived xenograft tumor models to study the role of CCT2 *in vivo*. SAS cells infected with shCCT2 lentivirus or control lentivirus were inoculated i.c. in the left hind limb of nude mice and the tumors were collected at the 21th day post inoculation. Downregulation of CCT2 expression significantly inhibited the growth of tumor *in vivo*(Figure 4A&B). The tumor volume ( $224\pm 114\text{ mm}^3$ ) and weight ( $622\pm 195\text{ mg}$ ) of the SAS-shCCT2-derived xenografts were significantly smaller ( $p<0.01$ ) than those of the SAS-control-derived xenografts ( $735\pm 347\text{ mm}^3$ ;  $1174\pm 309\text{ mg}$ ) (Figure 4C&D). Moreover, the expression of CCT2 in shCCT2-derived xenografts was still significantly lower than the control after growth of 21 days (Figure 4E).

### **Knockdown of CCT2 arrests cell cycle at G2 phase**

In order to explore the mechanism of the proliferation-promoting function of CCT2, we performed transcriptomic analysis for shCCT2 and control cells from SAS cell line. There were 536 differentially expressed genes (DEGs), of which 84 genes were upregulated and 452 were downregulated, respectively (fold change > 2 and adjusted  $p$  value < 0.05)(Figure 5A). The functions of CCT2 and the genes significantly associated with CCT2 alterations were then predicted by analyzing Gene Ontology (GO) and Kyoto Encyclopedia of Genes and Genomes (KEGG) analysis. GO analysis predicted the involvement of DEGs in biological process and molecular functions (Figure 5A). We found that signaling receptor binding and cellular protein metabolic process were significantly regulated by the CCT2 alteration in HNSCC. KEGG analysis defined the pathway related to the functions of CCT2 alteration and the frequently altered neighbor genes (Figure 5A). Cytokine-cytokine receptor interaction, PI3K-AKT signaling pathway, chemical carcinogenesis and rheumatoid arthritis were found to relate to the functions of CCT2 alteration and among which, PI3K-AKT signaling pathway was involved in the tumorigenesis and pathogenesis of HNSCC. Gene set enrichment analysis (GSEA) further supported the relation between CCT2 function and DNA replication and cell cycle (Figure 5B). Moreover, analysis with the GEPIA database indicated that CCT2 had positive correlation with CDK4 (Supplementary Figure S1A,  $r = 0.33$ ,  $p < 0.001$ ), CDK2 (Supplementary Figure S1B,  $r = 0.13$ ,  $p < 0.001$ ), CDK6 (Supplementary Figure S1C,  $r = 0.1$ ,  $p = 0.0052$ ), CDK7 (Supplementary Figure S1D,  $r = 0.17$ ,  $p < 0.001$ ) and Cdc20 (Supplementary Figure S1E,  $r = 0.21$ ,  $p < 0.001$ ), most of which were biomarkers of the G1-to-S phase transition.

We then analyzed the cell cycle and the results showed that knockdown of CCT2 increased the percentage of cells in G2 phase in both cell lines (Figure 5C), which indicated that CCT2 downregulation

caused arrest at G2 phase of cell cycle.

## **CCT2 regulates HNSCC cell proliferation via the Cdc20 mediated cyclin-CDK pathway**

To uncover the mechanism of CCT2 function on cell cycle, we further checked the key proteins important for cell cycles by western blot analysis. The results revealed that Cdc20 was significantly downregulated as well as CDK6, cyclinE1 and cyclinD1 in shCCT2 cells while CDK4 was increased (Figure 6A). Cdc20 is a regulator of cell division and requires CCT2 for stabilization, and can promote CDK4 degradation via the role of E3 ubiquitin-protein ligase[30]. CCT2 knockdown increased Cdc20 degradation thus enhanced CDK4 stability. Cdc20 degradation arrests cell cycle at G2 phase in HNSCC and modulated a series of cell cycle related proteins.

Next, we analyzed the protein level of CDK inhibitors such as p27, p21, and GSK3- $\alpha/\beta$ . Western blot analysis showed that GSK3- $\alpha/\beta$ , phosphorylated GSK3- $\beta$  (p-GSK3- $\beta$ ), phosphorylated p21 (p-p21) were increased while p21 was not affected in shCCT2 cells compared to the control cells (Figure 6B). GSK3- $\beta$  is well known for its suppressive function on cyclin D1 and E1 protein level by downregulating mRNA transcription and protein stability[31]. Both p21 and p27 protein are members of the Cip/Kip family of cyclin-dependent kinase (CDK) inhibitors that can inhibit kinase activities of CDK2-cyclin E complex, CDK4/6-cyclin D complex, and other cyclins[32, 33]. Enhancement of p27 protein level may cause G1 arrest[34]. Further study demonstrated the decreased transcription level of downstream factors such as cyclin E, E2F, and c-Myc (Figure 6C).

Taken together, considering that CCT2 is essential for Cdc20-dependent cell cycle events such as sister chromatid separation and exit from mitosis[35], the G2 arrest in CCT2 deficient cells could be explained by the facts of downregulation of both stability and function of Cdc20, which may cause upregulation of GSK3- $\alpha/\beta$  and p27, and the downregulation of cyclin D1, cyclin E1, and CDK6 (Figure 7).

## **Discussion**

### **Functions of CCT proteins**

CCT proteins are first known to be a chaperone required in the folding of actin and tubulin, the two major cytoskeletal proteins that are indispensable for the formation of mitotic spindle and the segregation of sister chromatids during cell division[36]. CCT family comprises eight different subunits. Depletion of either CCT1[15], CCT2[37], CCT3[17], CCT4[38], CCT5[39], CCT6[40], CCT7[41] or CCT8[18] led to growth arrest of tumor cells. When a CCT subunit became the target for depletion, the level of assembled oligomer reduced while more non-targeted subunits presented as monomers[10, 42]. Therefore, the CCT subunit depletion might disrupt the function of CCT oligomer as well as the specific function of certain CCT subunits in the monomeric forms. Considering that the targeting of several CCT subunits had similar influence on the proliferation of tumor cells, such effect probably resulted from the block of CCT oligomer function rather than a monomer-related function. As the function of CCT oligomer can be inhibited by

depleting the subunit, it provided a potential for CCT to be a viable therapeutic intervention target in cancers.

The role of CCT in cancers or other diseases is still far from fully characterized. First, Some CCT subunits may have unique monomeric activities, which called out challenges for the study of the chaperonin's function and regulation. For example, CCT5 promoted actin translation through cell surface signaling when there was already sufficient CCT oligomer for actin folding[42]. The monomeric function of CCT2 has few exploration. In breast cancer, silencing CCT2 expression resulted in the reduction of other CCT subunits while over-expressing CCT2 concomitantly increased other subunits[43]. Then, whether CCT has a broad range or rather restricted substrate is always the hot topic. Considering the complexity of the CCT binding interface and subunit-substrate interactions, many believe CCT has a rather discrete multiple folding substrates in which actin and tublin are the representatives[36]. Besides, lots of studies demonstrate the upregulation of CCT subunits in cancers and their role to promote cancer growth, but the mechanisms by which CCT subunits expression were modulated were poorly understood. And it's also unclear that whether cancer cells would be more susceptible to chaperonin inhibiting therapy than normal cells. There were also some limitations in this study. We detected the expression and function of CCT2 in HNSCC but no other subunits, so we could not verify the effect of CCT2 silencing on HNSCC is oligomer-driven, monomer-driven or both. HNSCC concludes various subtypes derived from different anatomic sites, which may different prognoses and therapeutic response. The main cancer cell lines used in the study, SAS and HSC-3 were both derived from tongue. And the number of HNSCC patients involved in the clinical characteristic observation is rather limited.

## **Function of CCT2 in cancer cell proliferation**

CCT proteins are found to involve in tumorigenesis of many types of cancers, but their role in HNSCC lacks exploration. A prediction of the expression and prognostic value of CCTs in HNSCC analyzing public online database aroused our interest, but the results need experimental evidences to be supported[28]. In this study, we found that CCT2 was upregulated in HNSCC and correlated with poor prognosis in patients through GEPIA website, which was in accordance with the previously mentioned study[28]. This result was further verified by the immunohistochemistry results of 41 samples of HNSCC patients and high expression level of CCT2 was significantly positively associated with the TNM classification. Our further study showed that the depleting CCT2 significantly slowed down the cell proliferation and invasiveness. And knockdown of CCT2 in HNSCC cells implanted to the nude mice impaired tumor growth. These results indicate that CCT2 is essential for cancer cell to survive and grow.

## **Function of CCT2 in cancer cell migration and invasion**

CCT has been reported to influence cell migration and invasion of a series of cancers in the previous articles[15–23]. In our study, CCT2 was proved to promote the migration and invasion capability of HNSCC as expected. The migration or invasion of both normal cell and cancer cell rely on actin filament rearrangement, and actin inquires interaction with the CCT oligomer for folding[10]. Besides, two actin-regulating proteins, the p21-activating kinase PAK4[44] and gelsolin[45], are known to bind CCT and are

implicated in cancer cell migration. EMT is a key pathway involved in tumor cell metastasis[46], and CCT2 knockdown led to significant change of the expression of EMT-associated proteins. Our results also implicated that CCT monomer can also function in mediating cell migration. Other CCT monomers have similar functions as well, for example, CCT3 and CCT4 were found to upregulated in cells that were able to migrate away from a tumor into Matrigel[47]. And the CCT4 monomer may have contrary influence on migration in different expression levels[48].

## Function of CCT2 in cell cycle

CCT subunits are upregulated in S phase of the cell cycle and the expression level are linked to cell growth, in accordance with the increase of tubulin synthesis around the G1/S transition[49]. Except for the CCT-tubulin interactions, CCT also interacts with some key cell cycle mediators like Cdc20, Cdh1, CDK2/cyclin E and polo-like kinase1 (PLK1). Cdc20 and Cdh1, both obligate CCT folding substrates, activate the APC/C (anaphase-promoting complex) during G1 phase and the transition from metaphase to anaphase[35]. And the maturation of cyclin E also requires the function of CCT[9]. PLK1 is important in the G2 phase of the cell cycle and a possible folding substrate and interaction partner of CCT[50]. Besides, CCT is reported to mediate the release of Cdc20 from mitotic checkpoint complex (MCC) to promote MCC disassembly and subsequently initiate the anaphase[51].

Our western blot results showed the downregulation of CDK6, cyclinD1, cyclin E1 and Cdc20 while upregulation of GSK3- $\alpha/\beta$  and p27 in CCT2 knockdown cells that show G2 arrest in cell cycle, which may partly explain how CCT2 promotes cell growth (Fig. 7). However, it remains unclear how CCT2 influences the level of these proteins. The decrease of cyclin D1 and E1 may be explained by the upregulation of GSK3- $\alpha/\beta$  but it cannot exclude the possibility that knockdown of CCT2 alters the correct folding of such cyclins. Higher phosphorylated GSK3- $\alpha/\beta$  suggest higher activities of kinases like Akt and PDK-1, and lower ubiquitination-based proteasome degradation which may be also the mechanism causing higher p27 protein. Gene expression profiling and bioinformatics analysis were of great potential to predict diagnostic and therapeutic targets in cancers. GEPIA website showed the upregulation and prognostic effect of CCT2 in HNSCC, which was then confirmed by experiments. When looking into the underlying mechanism of the function of CCT2 in HNSCC, the study of RNA-seq identified the DEGs and prompted that PI3K-AKT signaling pathway was enriched in the KEGG pathway analysis, which was in accordance with the results from the public database. Western blot further verified the alteration of PI3K-AKT pathway when CCT2 was knockdown. Further analysis of proteomics such as iTRAQ may provide better explanation of CCT2 function on proteins of cell cycle and PI3K-AKT pathway than transcriptome analysis since the main direct function of CCT2 is protein folding.

## Conclusion

The expression of CCT2 in HNSCC is remarkably upregulated and therefore promote HNSCC progression through accelerating cell proliferation via cyclin-CDK pathway. High level of CCT2 is a poor prognostic factor for HNSCC patients and may serve as a potential therapeutical target of HNSCC.

# Materials And Methods

## Patients and follow-up

A total of 41 HNSCC patients underwent surgical resection at the Department of Craniofacial Surgery, Guanghua School of Stomatology, Sun Yat-sen University (Guangzhou, China) from January 2017 to December 2017 were enrolled in the study. Before the surgery, no one had received radiotherapy or chemotherapy. Primary HNSCC tissues were obtained from the representative area of each case, verified by pathological examination. The paraffin-embedded HNSCC and matched peritumor tissues were collected for immunohistochemistry. Informed consent from patients was obtained and their medical records were reviewed for clinical information. Ethical approval of the study was obtained from the Ethics Committee of Guanghua School of Stomatology, Sun Yat-sen University.

## GEPIA (Gene Expression Profiling Interactive Analysis) dataset

GEPIA (<http://gepia.cancer-pku.cn/>) is an interactive web used for analyzing RNA sequencing expression data from The Cancer Genome Atlas (TCGA) and Genotype-Tissue Expression project (GTEx), with a standard processing pipeline. The website provides customizable functions like tumor/normal tissue differential expression analysis and patient survival analysis. The raw data of unpaired normal and tumor tissues were compared and filtered based on the cutoffs  $|\log_2FC| > 1$  and  $P < 0.01$ . The  $\log_2(TPM + 1)$  transformed expression data were shown in plots or used for one-way ANOVA analysis. While analyzing the overall survival (OS) and disease-free survival (DFS) of patients with HNSCC, patient samples were divided into two groups by median expression (high/low expression) and then shown in a Kaplan-Meier survival plot, with the hazard ratio (HR) with 95% confidence intervals (CI) and logrank p value.

## Immunohistochemistry

Tissue sections from paraffin-embedded HNSCC patient tissue or SAS xenograft model were dewaxed in xylene and rehydrated in a graded alcohol series. Next the sections were soaked with 0.1% Trion X-100, incubated in 3%  $H_2O_2$  in order to eliminate endogenous peroxidase activity and then heated in sodium citrate buffer (pH 6.0) for antigen retrieval. After blocking in 10% goat serum for 1h at room temperature, the sections were incubated with CCT2 primary antibody overnight at 4°C. Washed with PBST, the sections were incubated with secondary antibody for 1h at room temperature and visualized with DAB solution and counterstained with hematoxylin. The expression of CCT2 was scored by two pathologists respectively. The ratio of positively stained cells < 25% was negative, 25%-50% was +, 50%-75% was ++ and > 75% was +++.

## Cell culture and transfection

The human HNSCC cell lines CAL-27 were purchased from ATCC (Rockville, MD, USA), and the cell lines HSC-3 and HSC-6 were provided by J. Silvio Gutkind (NIH, Bethesda, MD, USA). Cell lines SAS and NOK

was purchased from Fuheng Biology (Shanghai,China). Cells were mycoplasma-free and were cultured under the recommended conditions.

The vectors of pLKO.1-TRC-puromycin-shRNA-CCT2 and pLKO.1-TRC-puromycin were constructed and transfected into SAS and HSC-3 cells, according to the manufacturer's instruction. The shRNA1 sequence is TTATCGAGGAAGTCATGATTG. The shRNA2 sequence is GCCTCTCTTATGGTAACCAAT. The transfected cells were screened with puromycin at a concentration of 3 $\mu$ g/ml for SAS and HSC-3 cell lines. The transfection efficiency was verified by qRT-PCR and western blotting.

### **Real-time reverse transcription PCR(qRT-PCR) and western blot analysis**

For total protein extraction, cells lysates were collected using RIPA buffer (Sigma-Aldrich) supplemented with protease and phosphatase inhibitors. 20 $\mu$ g of total protein were loaded into 10% SDS-PAGE gel for separation and transferred to a PVDF membrane (Millipore, MA, USA). The PVDF membranes were blocked with 5% milk for 1h and then incubated with primary antibodies at 4 °C overnight. Next the membranes were incubated with the secondary antibody for 1h. The bands was visualized using the enhanced chemiluminescence (ECL) detection system (Millipore, MA, USA). All the primary antibodies are listed in Supplementary Table S1.

Total RNA was extracted from cell lines with TRIzol (Invitrogen, Carlsbad,

CA, USA) and reverse-transcribed to cDNA with Hifair<sup>TM</sup> III 1<sup>st</sup> Strand cDNA Synthesis SuperMix for qPCR(Yeasen, SH, China). qRT-PCR was performed using SYBR Green Master Mix Kit (Yeasten) on a Light Cycler 480 system (Roche).The qRT-PCR primers are shown in Supplementary Table S2. The results were normalized to those for GAPDH.

### **CCK-8, EdU and colony formation assays**

shCCT2 cells and control cells were inoculated into 96-well plates(3000 cells/well). 10 $\mu$ l of CCK-8 solution (Dojindo, Kumamoto, Japan) was added into the sextuplicate wells At each time point(24, 48, 72 and 96 h). After incubating for 1h, the absorbance was detected at 450nm.

The EdU incorporation assay is designed to quantitate cell proliferation based on the measurement of EdU incorporation during DNA synthesis in proliferating cells. The developed color correlates with the number of proliferating cells in the respective microcultures. The assay was performed with the Cell Proliferation EdU Image Kit (Green Fluorescence) (Abbkine, CA, USA) according to the manufacturer's instruction.

The colony formation assay was used to test the cell proliferation capacity as well. Cells were seeded in 6-well plates(1000cells/well) with culture medium refreshed twice a week. After 10-14 days, the cells was fixed with 4% formaldehyde and then stained with crystal violet. Colonies containing >10 cells was counted manually.

## **Transwell and wound healing**

Transwell assay was performed to detect cell migration and invasion. In brief, SAS and HSC-3 cells ( $1 \times 10^5$ ) were suspended in 200  $\mu$ l serum-free medium and added into the upper compartments of 24-well Transwell chambers (8  $\mu$ m pore size; Corning, NY, USA) after transfection. 600  $\mu$ l of complete medium containing 10% FBS was filled into the lower compartment. After co-culturing for 24-48h, the cells remained in the upper compartments were removed with cotton buds and the cells translocated to the lower compartments were fixed in 4% paraformaldehyde and stained 0.1% crystal violet. Under an optical microscope (Carl Zeiss), photographs of randomly selected five visual fields of each well were captured for analysis. For Boyden assays, the procedure was similar except the Transwell membranes were pre-coated with 24  $\mu$ g/ml Matrigel (R&D Systems, Minneapolis, MN, USA).

As to the wound healing assay, HNSCC cells were seeded in 6-well plates, cultured overnight and then scratched by a sterile plastic tip with 95% confluence rate. After washing with PBS for three times, the cells were cultured with serum-free medium for 24-48 h. Under an optical microscope (Carl Zeiss), photographs of randomly selected fields across three replicate wells were captured for analysis.

## **Flow cytometric analysis**

Flow cytometric analysis was used to detect cell cycle and apoptosis. Cells were stained with Cell Cycle Staining Kit (Lianke, HZ, China) according to the manufacturer's instructions. Stained cells were detected by flow cytometry (BD Biosciences, Franklin Lakes, NJ, USA) and analyzed by FlowJo software version 10.

## **RNA-seq**

Total RNA of transfected SAS cells was purified as described above. mRNA was enriched with oligo (dT)-attached magnetic beads and fragmented into pieces. First-strand cDNA was developed using random hexamer-primed reverse transcription. Then second-strand cDNA was synthesized and sequenced on an MGI 2000 platform (BGI, Shenzhen, China). The clean reads were then mapped to the human reference genome (mm10) with STAR v1.5.1. Gene expression level was quantified with HTSeq-count v0.11.3. DEGs were analyzed with the default settings of the DESeq2 v1.28.1 algorithm and the significant ones were set a false discovery rate of  $<0.05$  and a fold change of  $>2$ . The following processing and visualization of the data were performed by Dr. Tom platform (BGI, Shenzhen, China). The RNA-seq data are deposited in GEO database (Access No. GSE195850)

## **In vivo tumorigenesis**

Xenograft experiments in nude mice were approved by the Ethics Committee of the Hospital of Stomatology, Sun Yat-sen University. The animal experiments were complied with the stated guidelines of 3Rs (replacement, reduction, and refinement). Male mice aged from 4-6 weeks of BALB/c nude mice were randomly divided into two subgroups ( $n=7$  for each group): control group (Vector) and treatment group

(shRNA).  $5 \times 10^6$  cells (per mouse) suspended in 100 $\mu$ l PBS were injected to subcutaneous space of left waist of nude mice. Tumor growth was monitored every three days. Animals were sacrificed after 21 days. Tumor tissues were fixed in formalin and embedded in paraffin for immunohistochemistry. The tumor volume was measured following the formula : $V = \pi/6 \times (\text{larger diameter}) \times (\text{smaller diameter})^2$ .

## Statistical analysis

All experiments were performed in triplicate. Data are presented as the mean  $\pm$ SD. Student's t-test was used for comparison between two groups. One-way ANOVA (no matching) was used for comparison between multiple groups. Categorical data were analyzed with the chi-square test or Fisher's exact test. The data was analyzed using SPSS 23.0 software (IBM, Armonk, NY, USA) and performed by GraphPad Prism 5.0 (GraphPad software, San Diego, CA, USA). A two-tailed P value  $<0.05$  was considered statistically significant.

## Declarations

**Acknowledgements** We are grateful to facilities of Institution of Stomatological Research of Sun Yat-sen University for technical assistance.

**Conflict of interest** The authors declare that they have no conflict of interest.

**Author Contributions** **Lin Lu**: Conceptualization, Methodology, Investigation, Writing-Original draft preparation; **Xurong Li**: Investigation, Software; **Yiwei Zhao**: Data curation, Validation; **Xuefan Zhai**: Visualization, Investigation; **Min Cai**: Methodology, Resources; **Baicheng Bao**: Supervision; **Menghuan Li**: Validation, Resources; **Jianbo Sun**: Conceptualization, Supervision, Writing-Reviewing and Editing.

**Funding** Funding This work is supported by Guangdong Basic and Applied Basic Research Foundation (Grant No. 2022A1515010678 and 2021A1515012324) to J.S.; Guangzhou Basic and Applied Basic Research Foundation (202002030127) to J.S. Fundamental Research Funds for the Central Universities (20ykzd08) to J.S.; Natural Science Foundation of Guangdong Province (2018A030313563) to J.S.

**Compliance with ethical standards** All institutional and national guidelines for the care and use of laboratory animals were followed. This study was performed in line with the principles of the Declaration of Helsinki. Approval was granted by the Medical Ethics Committee of Hospital of Stomatology, Sun Yat-Sen University (No. [2020]000932 & No. KQEC-2021-76-01).

**Availability of Data and Materials** All data generated or analyzed during this study are included in this published article and its supplementary information files. Supplementary information is available at Cellular Oncology website at the end of the article and before the references.

## References

1. A. Argiris, C. Eng, Epidemiology, Staging, and Screening of Head and Neck Cancer. *Cancer Treat. Res.* **114**(114), 15 (2003)
2. J. Ferlay et al., Cancer incidence and mortality worldwide: Sources, methods and major patterns in GLOBOCAN 2012. *Int. J. Cancer* **136**(5), E359–E386 (2015)
3. B. Yang et al., Progresses and Perspectives of Anti-PD-1/PD-L1 Antibody Therapy in Head and Neck Cancers. *Front. Oncol.* **8**, 563 (2018)
4. L. Ditzel et al., Crystal structure of the thermosome, the archaeal chaperonin and homolog of CCT. *Cell* **93**(1), 125–138 (1998)
5. M.A. Kabir et al., Functional Subunits of Eukaryotic Chaperonin CCT/TRiC in Protein Folding. *J. amino acids* **2011**, 843206–843206 (2011)
6. L.A. Joachimiak et al., The Structural Basis of Substrate Recognition by the Eukaryotic Chaperonin TRiC/CCT. *Cell* **159**(5), 1042–1055 (2014)
7. S. Kim, K.R. Willison, A.L. Horwich, Cytosolic chaperonin subunits have a conserved ATPase domain but diverged polypeptide-binding domains. *Trends Biochem. Sci.* **19**(12), 543–548 (1994)
8. A.Y. Yam et al., Defining the TRiC/CCT interactome links chaperonin function to stabilization of newly made proteins with complex topologies. *Nat. Struct. Mol. Biol.* **15**(12), 1255–1262 (2008)
9. K.-A. Won et al., Maturation of human cyclin E requires the function of eukaryotic chaperonin CCT. *Mol. Cell. Biol.* **18**(12), 7584–7589 (1998)
10. H. Sternlicht et al., The t-complex polypeptide 1 complex is a chaperonin for tubulin and actin in vivo. *Proc. Natl. Acad. Sci. U.S.A.* **90**(20), 9422–9426 (1993)
11. R. Melki et al., Cytoplasmic chaperonin containing TCP-1: Structural and functional characterization. *Biochemistry* **36**(19), 5817–5826 (1997)
12. W.J. Hansen et al., Diverse effects of mutations in Exon II of the von Hippel-Lindau (VHL) tumor suppressor gene on the interaction of pVHL with the cytosolic chaperonin and pVHL-dependent ubiquitin ligase activity. *Mol. Cell. Biol.* **22**(6), 1947–1960 (2002)
13. A.G. Trinidad et al., Interaction of p53 with the CCT Complex Promotes Protein Folding and Wild-Type p53 Activity. *Mol. Cell* **50**(6), 805–817 (2013)
14. M. Kasembeli et al., *Modulation of STAT3 Folding and Function by TRiC/CCT Chaperonin*. *Plos Biology*, 2014. 12(4)
15. S.T. Guest et al., Two members of the TRiC chaperonin complex, CCT2 and TCP1 are essential for survival of breast cancer cells and are linked to driving oncogenes. *Exp. Cell Res.* **332**(2), 223–235 (2015)
16. R. Bassiouni et al., Chaperonin Containing TCP-1 Protein Level in Breast Cancer Cells Predicts Therapeutic Application of a Cytotoxic Peptide. *Clin. Cancer Res.* **22**(17), 4366–4379 (2016)
17. X. Cui et al., Overexpression of chaperonin containing TCP1, subunit 3 predicts poor prognosis in hepatocellular carcinoma. *World J. Gastroenterol.* **21**(28), 8588–8604 (2015)

18. X.D. Huang et al., Chaperonin containing TCP1, subunit 8 (CCT8) is upregulated in hepatocellular carcinoma and promotes HCC proliferation. *Apmis* **122**(11), 1070–1079 (2014)
19. Y.Y. Zhang et al., Molecular chaperone CCT3 supports proper mitotic progression and cell proliferation in hepatocellular carcinoma cells. *Cancer Lett.* **372**(1), 101–109 (2016)
20. C. Coghlin et al., Characterization and over-expression of chaperonin t-complex proteins in colorectal cancer. *J. Pathol.* **210**(3), 351–357 (2006)
21. Q.L. Zhu et al., Inhibition of Cytosolic Chaperonin CCT zeta-1 Expression Depletes Proliferation of Colorectal Carcinoma In Vitro. *J. Surg. Oncol.* **102**(5), 419–423 (2010)
22. L.J. Li et al., Chaperonin containing TCP-1 subunit 3 is critical for gastric cancer growth. *Oncotarget* **8**(67), 111470–111481 (2017)
23. A.C. Carr et al., Targeting chaperonin containing TCP1 (CCT) as a molecular therapeutic for small cell lung cancer. *Oncotarget* **8**(66), 110273–110288 (2017)
24. S.H. Roh et al., Chaperonin TRiC/CCT Modulates the Folding and Activity of Leukemogenic Fusion Oncoprotein AML1-ETO. *J. Biol. Chem.* **291**(9), 4732–4741 (2016)
25. E.N. Qian et al., *Expression and diagnostic value of CCT3 and IQGAP3 in hepatocellular carcinoma.* *Cancer Cell International*, 2016. 16
26. S. Hallal et al., Extracellular Vesicles from Neurosurgical Aspirates Identifies Chaperonin Containing TCP1 Subunit 6A as a Potential Glioblastoma Biomarker with Prognostic Significance. *Proteomics* **19**(1–2), e1800157 (2019)
27. S.H. Park et al., Activating CCT2 triggers Gli-1 activation during hypoxic condition in colorectal cancer. *Oncogene* **39**(1), 136–150 (2020)
28. Y.B. Dong et al., CCTs as new biomarkers for the prognosis of head and neck squamous cancer. *Open Med.* **15**(1), 672–688 (2020)
29. J. Doescher, J.A. Veit, T.K. Hoffmann, The 8th edition of the AJCC Cancer Staging Manual. Updates in otorhinolaryngology, head and neck surgery. *Hno* **65**(12), 956–956+ (2017)
30. Q. Wang et al., Cdc20 and molecular chaperone CCT2 and CCT5 are required for the Muscovy duck reovirus p10.8-induced cell cycle arrest and apoptosis. *Vet. Microbiol.* **235**, 151–163 (2019)
31. S. Xu et al., 6-Gingerol induces cell-cycle G1-phase arrest through AKT-GSK 3 beta-cyclin D1 pathway in renal-cell carcinoma. *Cancer Chemother. Pharmacol.* **85**(2), 379–390 (2020)
32. A.J. Massey et al., Targeting DYRK1A/B kinases to modulate p21-cyclin D1-p27 signalling and induce anti-tumour activity in a model of human glioblastoma. *J. Cell. Mol. Med.* **25**(22), 10650–10662 (2021)
33. H.Y. Sun et al., *Anti-Cancer Activity of Catechin against A549 Lung Carcinoma Cells by Induction of Cyclin Kinase Inhibitor p21 and Suppression of Cyclin E1 and P-AKT.* *Applied Sciences-Basel*, 2020. 10(6)
34. T. Okumura, Mechanisms by which thiazolidinediones induce anti-cancer effects in cancers in digestive organs. *J. Gastroenterol.* **45**(11), 1097–1102 (2010)

35. A. Camasses et al., The CCT chaperonin promotes activation of the anaphase-promoting complex through the generation of functional Cdc20. *Mol. Cell* **12**(1), 87–100 (2003)
36. J. Vallin, J. Grantham, The role of the molecular chaperone CCT in protein folding and mediation of cytoskeleton-associated processes: implications for cancer cell biology. *Cell. Stress & Chaperones* **24**(1), 17–27 (2019)
37. A.E. Showalter et al., Investigating Chaperonin-Containing TCP-1 subunit 2 as an essential component of the chaperonin complex for tumorigenesis. *Sci. Rep.* **10**(1), 798 (2020)
38. W. Li, J. Liu, H. Zhao, *Prognostic Power of a Chaperonin Containing TCP-1 Subunit Genes Panel for Hepatocellular Carcinoma*, 12 (*Frontiers in Genetics*, 2021)
39. H. Gao, H. Wang, Y. Zhu, Identification of a Novel Tumor Associated Antigen in Non-small Cell Lung Cancer. *Bull. Chin. Cancer* **26**(5), 405–409 (2017)
40. G.F. Zeng et al., Overexpressing CCT6A Contributes To Cancer Cell Growth By Affecting The G1-To-S Phase Transition And Predicts A Negative Prognosis In Hepatocellular Carcinoma. *Oncotargets and Therapy* **12**, 10427–10439 (2019)
41. L. Wang et al., Clinical Significance, Cellular Function, and Potential Molecular Pathways of CCT7 in Endometrial Cancer. *Front. Oncol.* **10**, 1468 (2020)
42. K.I. Brackley, J. Grantham, Subunits of the chaperonin CCT interact with F-actin and influence cell shape and cytoskeletal assembly. *Exp. Cell Res.* **316**(4), 543–553 (2010)
43. A.E. Showalter et al., *Investigating Chaperonin-Containing TCP-1 subunit 2 as an essential component of the chaperonin complex for tumorigenesis*. *Scientific Reports*, 2020. 10(1)
44. M. Zhao et al., Identification of the PAK4 interactome reveals PAK4 phosphorylation of N-WASP and promotion of Arp2/3-dependent actin polymerization. *Oncotarget* **8**(44), 77061–77074 (2017)
45. K.I. Brackley, J. Grantham, Interactions between the actin filament capping and severing protein gelsolin and the molecular chaperone CCT: evidence for nonclassical substrate interactions. *Cell. Stress & Chaperones* **16**(2), 173–179 (2011)
46. Q. Fu et al., SHIP1 inhibits cell growth, migration, and invasion in non-small cell lung cancer through the PI3K/AKT pathway. *Oncol. Rep.* **41**(4), 2337–2350 (2019)
47. W.G. Wang et al., Identification and testing of a gene expression signature of invasive carcinoma cells within primary mammary tumors. *Cancer Res.* **64**(23), 8585–8594 (2004)
48. M. Echbarhi, J. Vallin, J. Grantham, Interactions between monomeric CCTS and p150(Glued): A novel function for CCTS at the cell periphery distinct from the protein folding activity of the molecular chaperone CCT. *Exp. Cell Res.* **370**(1), 137–149 (2018)
49. S. Yokota et al., Cytosolic chaperonin is up-regulated during cell growth - Preferential, expression and binding to tubulin at G(1)/S transition through early S phase. *J. Biol. Chem.* **274**(52), 37070–37078 (1999)
50. X.Q. Liu et al., CCT chaperonin complex is required for the biogenesis of functional Plk1. *Mol. Cell. Biol.* **25**(12), 4993–5010 (2005)

51. S. Kaisari et al., Role of CCT chaperonin in the disassembly of mitotic checkpoint complexes. Proc. Natl. Acad. Sci. U.S.A. **114**(5), 956–961 (2017)

## Tables

Table 1. Association between immunohistochemical expression of CCT2 and clinicopathological characteristics (n =41)

	CCT2 expression		Significance
	Negative	Positive	P value
Age			0.443
≤ 60(years)	8	22	
≥60(years)	5	6	
Gender			0.993
Female	4	7	
Male	9	21	
Tumor size			0.059
T1/T2	12	16	
T3/T4	1	12	
Node category			0.103
N <sup>-</sup>	10	14	
N <sup>+</sup>	3	14	
Pathology differentiation			0.344
Well	4	13	
Moderate/Poor	9	15	
TNM classification			<b>0.014*</b>
I/II	10	10	
III/IV	3	18	
Cigarette			0.756
Yes	10	18	
No	4	9	
Alcohol (>5g/Day)			0.343
Yes	7	21	
No	2	11	
Prognosis			0.608

Well	8	21
Poor	5	7

## Figures

Fig.1

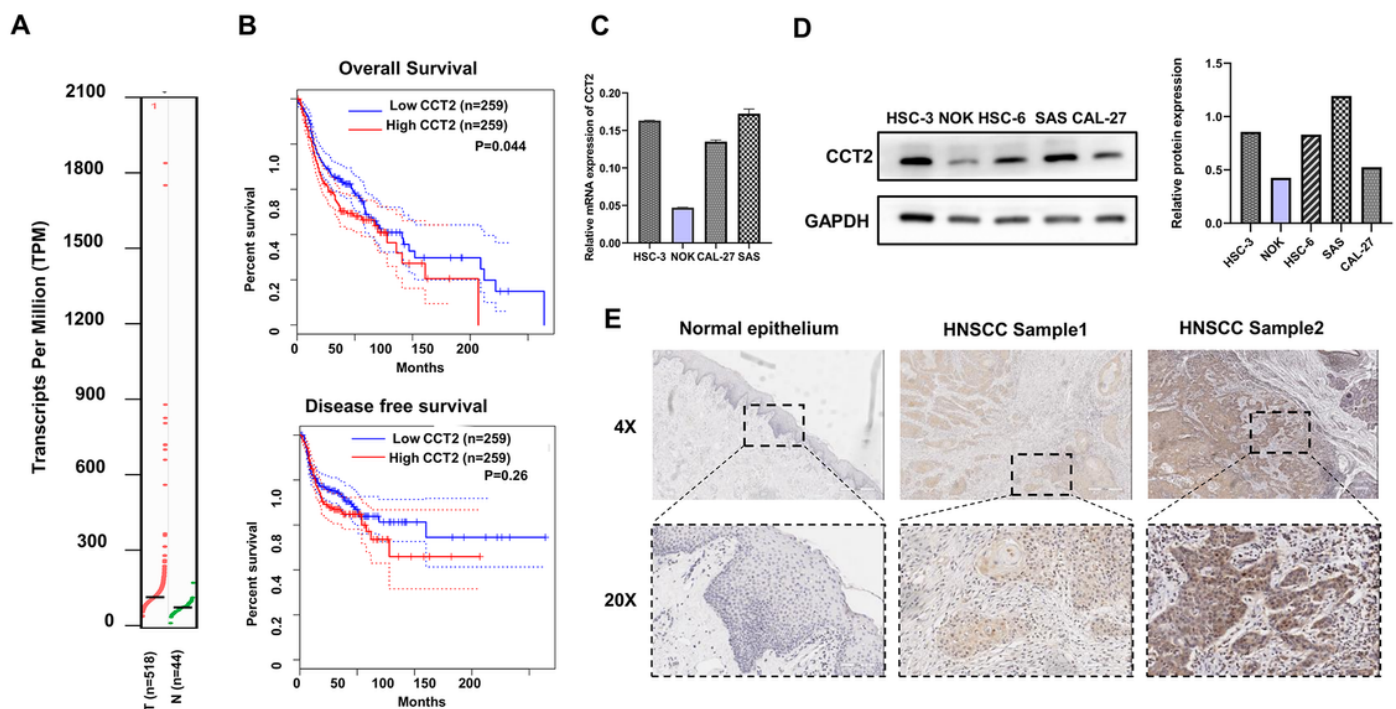


Figure 1

The expression of CCT2 was significantly upregulated in HNSCC and high expression level of CCT2 was associated with worse clinical outcomes. **A** Transcriptional level of CCT in tumor tissues and normal tissues. **B** Correlation of overall survival and disease-free survival with CCT2 expression level. **C-D** CCT2 mRNA and protein expression in HNSCC cell lines and normal oral squamous cell line. **E** Representative images of the TMA stained with IHC for CCT2.

Fig.2

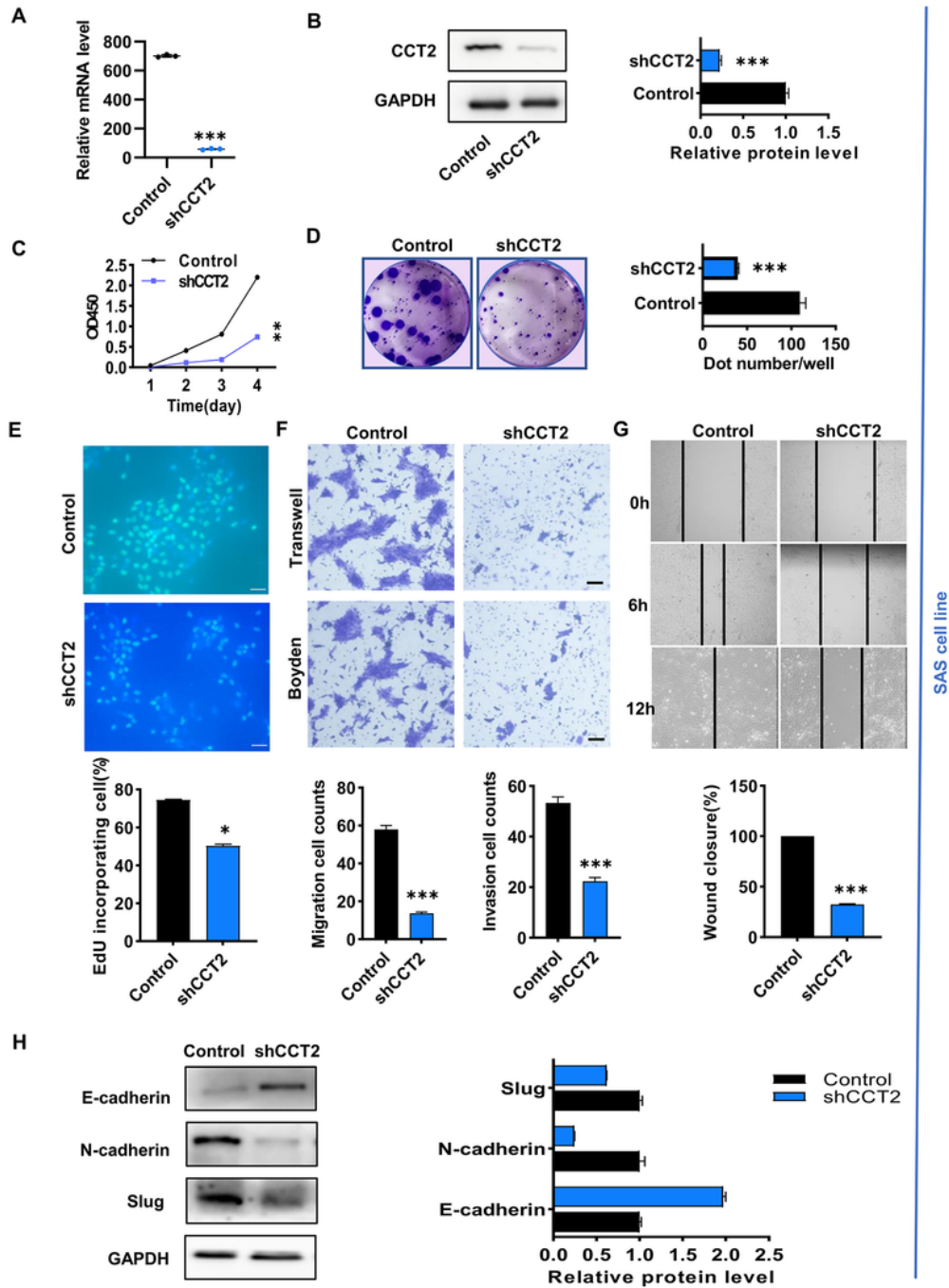


Figure 2

CCT2 promoted the proliferation, migration and invasion of HNSCC cells in vitro. **A-B** mRNA and protein level of CCT2 in SAS cell line after lentivirus transfection. **C-E** Interference with CCT2 expression in SAS cells inhibited cell proliferation determined by CCK-8, colony formation assays and EdU assays . **F-G**

knockdown of CCT2 significantly decreased the migration and invasion ability of SAS cells shown by wound healing, Transwell and Boyden assays. **H** Detection of the expression level of EMT related proteins. Scale bar, 50 $\mu$ m. \*  $p < 0.05$ ; \*\*  $p < 0.01$ ; \*\*\*  $p < 0.001$

Fig.3

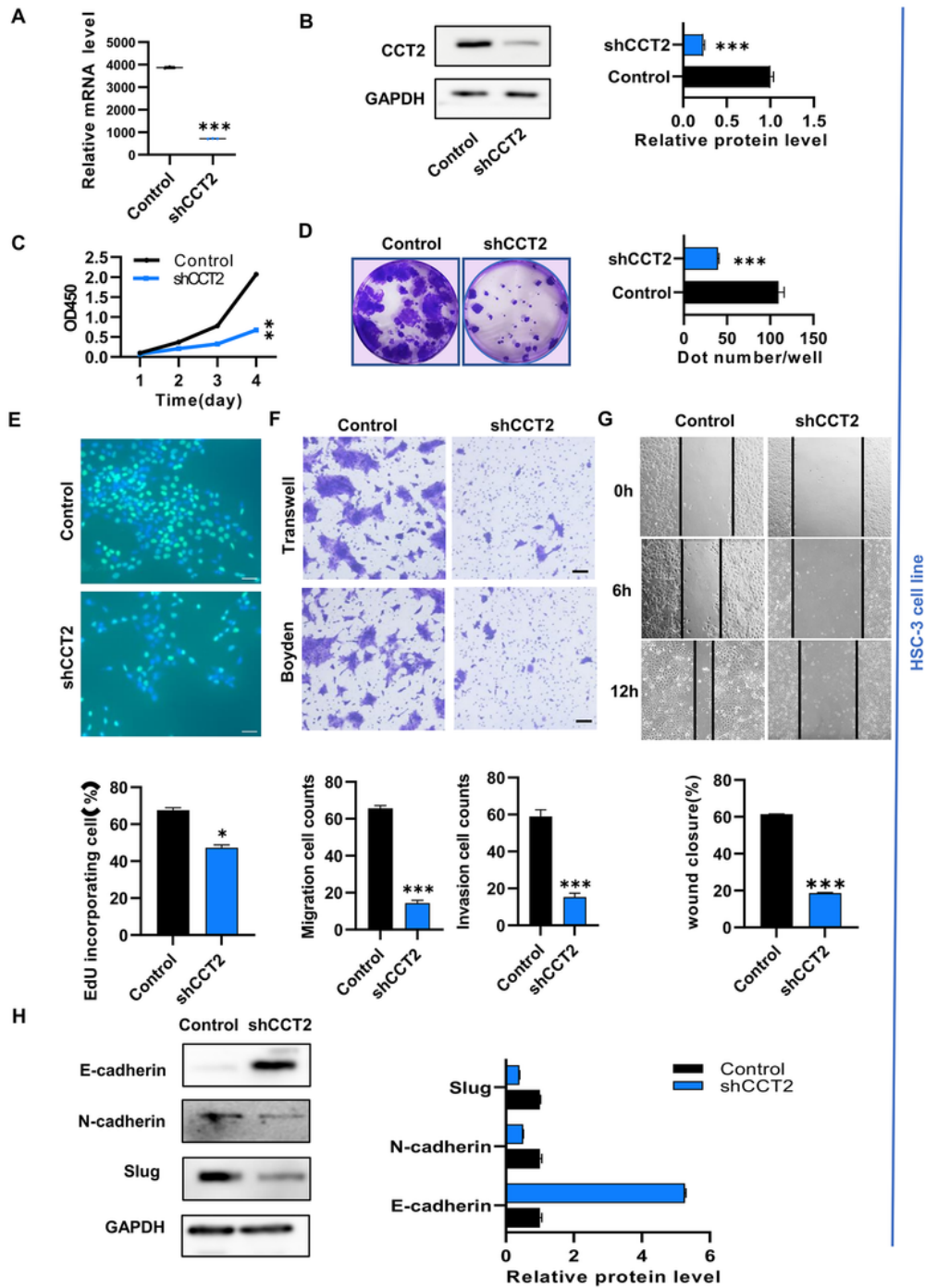
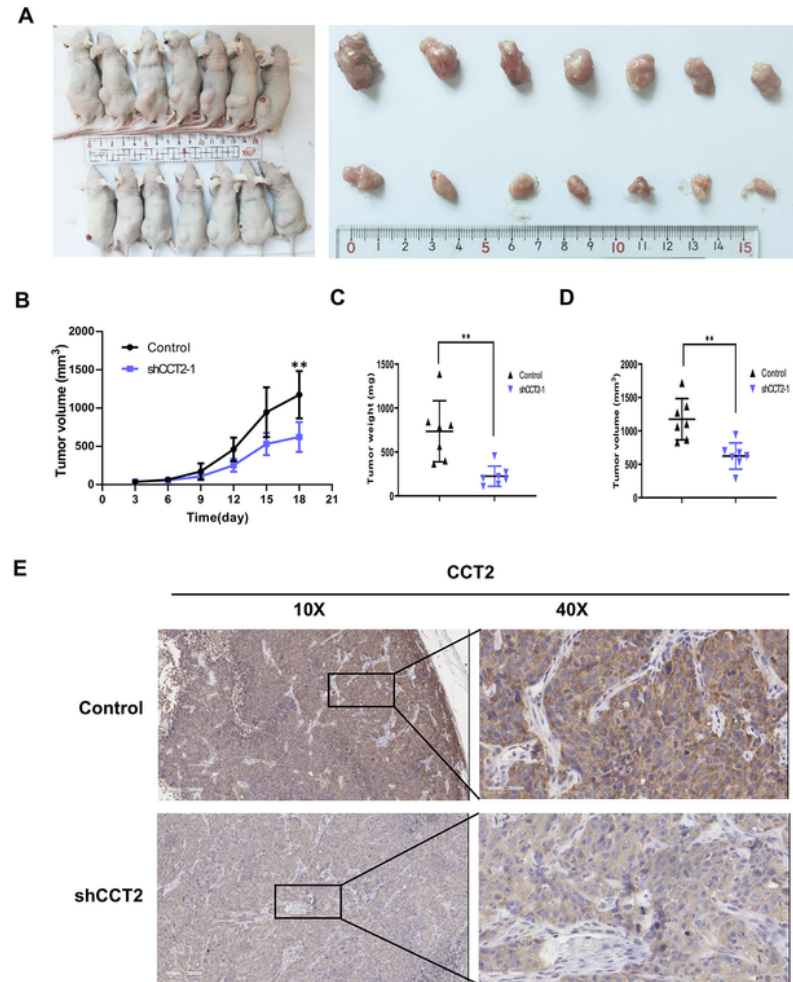


Figure 3

CCT2 promoted the proliferation, migration and invasion of HNSCC cells in vitro. **A-B** mRNA and protein level of CCT2 in HSC-3 cell line after lentivirus transfection. **C-E** Interference with CCT2 expression in HSC-3 cells inhibited cell proliferation determined by CCK-8, colony formation assays and EdU assays . **F-G** knockdown of CCT2 significantly decreased the migration and invasion ability of HSC-3 cells shown by wound healing, Transwell and Boyden assays. **H** Detection of the expression level of EMT related proteins. Scale bar, 50 $\mu$ m. \*  $p < 0.05$ ; \*\*  $p < 0.01$ ; \*\*\*  $p < 0.001$

Fig.4



**Figure 4**

Downregulation of CCT2 inhibited HNSCC cell growth in vivo. **A** Photos of Subcutaneous xenograft tumors at the 21th day. **B** Record curve of tumor volume. **C-D** The weights and volumes of the tumors at the 21th day. **E** Representative pictures of subcutaneous xenograft tumors stained with IHC. \*\*  $p < 0.01$

Fig.5

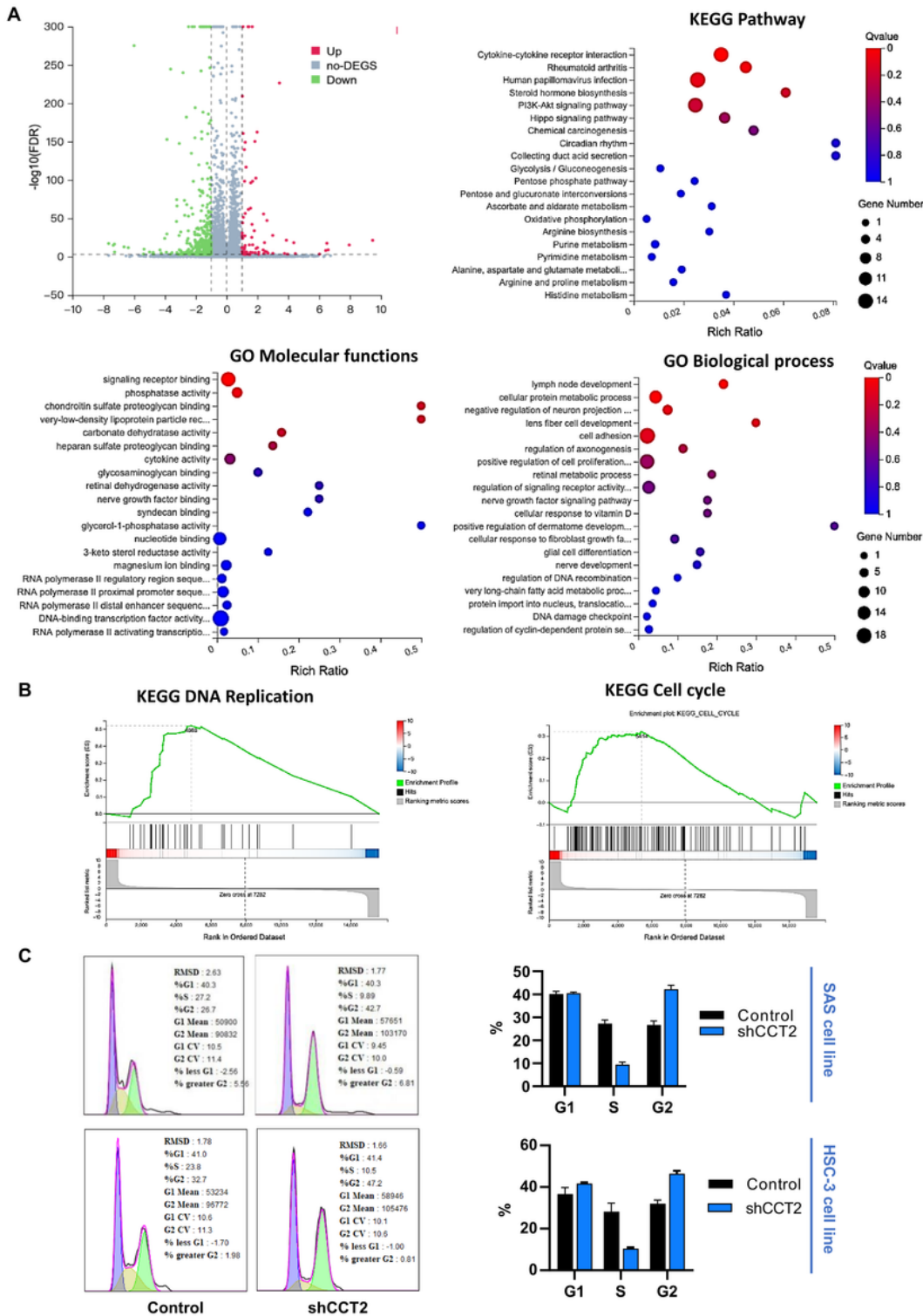
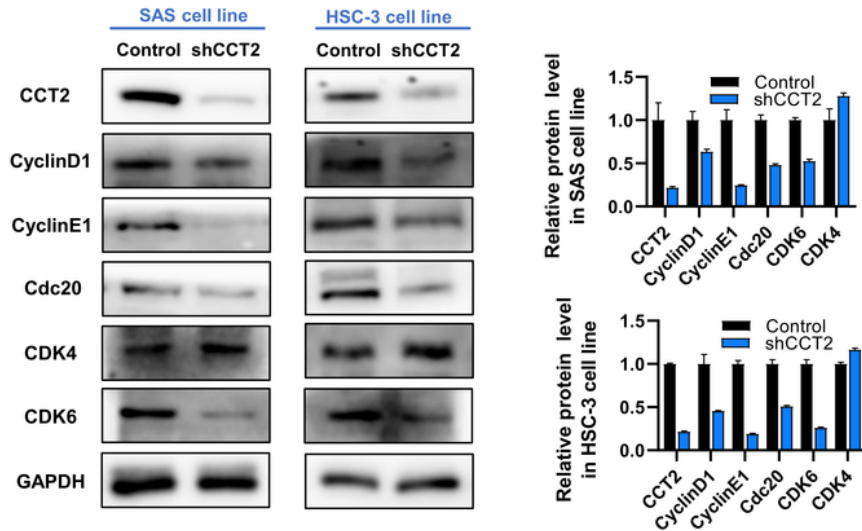


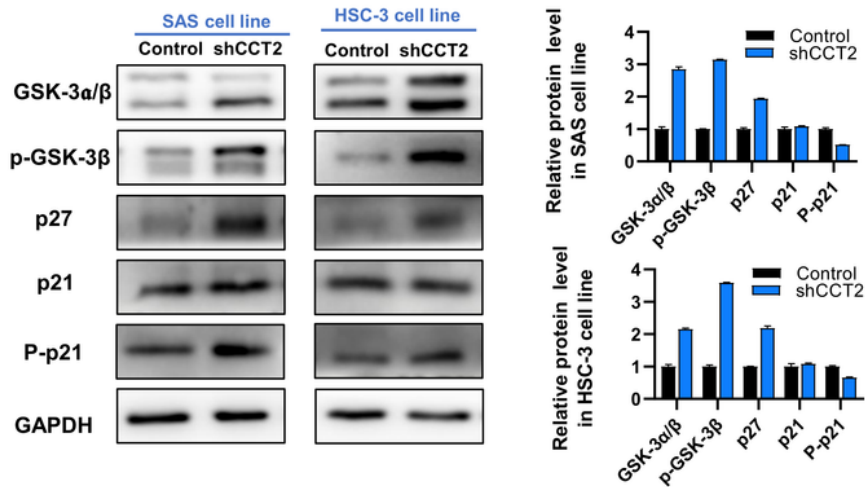
Figure 5

Downregulation of CCT2 arrested cell cycle at G2 phase. **A** DEGs identified as fold change >2 and  $p$  value of < 0.05, KEGG pathway analysis and Gene Ontology analysis. **B** Gene set enrichment analysis. **C** cell cycle analysis of the shCCT2 and control cells by flowcytometry.

Fig.6 A



B



C

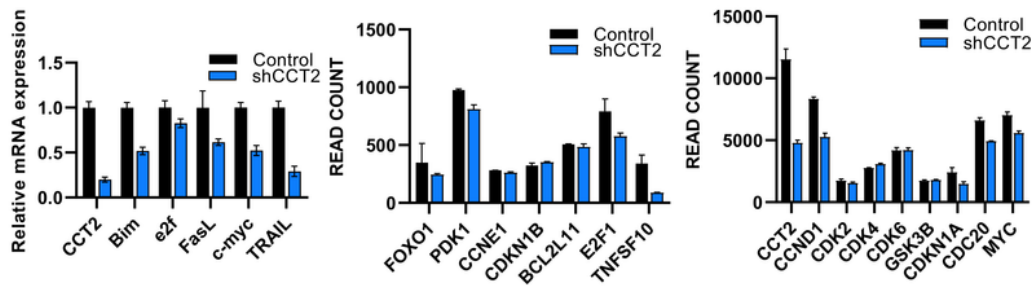


Figure 6

CCT2 regulated HNSCC cell proliferation through cyclin-CDK pathway. **A** Western blot bands for CCT2, Cyclin D1, Cyclin E1, Cdc20, CDK4, CDK6 for shCCT2 and control cells of SAS and HSC-3 cell line, respectively. **B** Western blot bands for GSK-3- $\alpha/\beta$ , p-GSK-3- $\beta$ , p27, p21 and p-p21 for shCCT2 and control cells of SAS and HSC-3 cell line, respectively. **C** mRNA level determined by RT-qPCR or read counts from

RNA-seq data for CCT2, Bim, e2f, FasL, c-myc, TRAIL, and some cell cycle related genes in shCCT2 and control cells of SAS cell line.

Fig.7

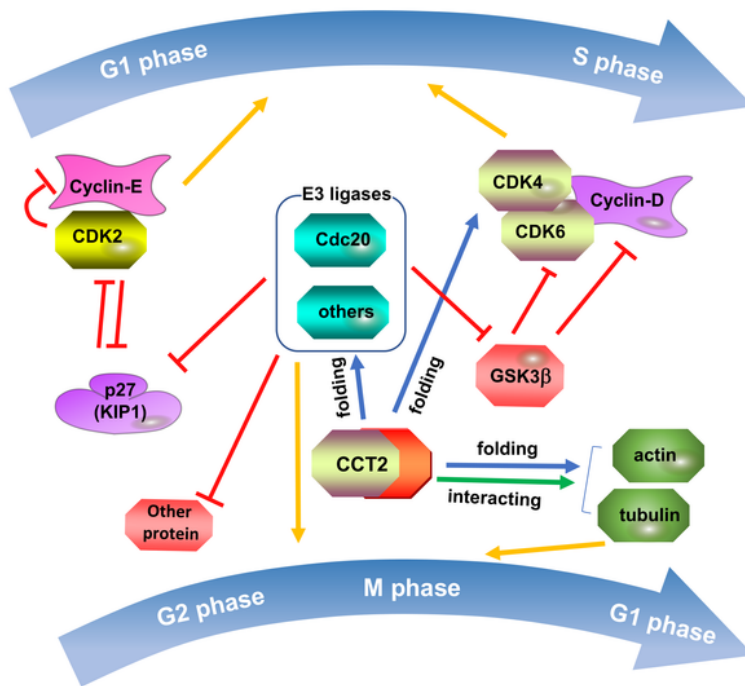


Figure 7

Schematic model illustrating the effect of CCT2 on Cdc20 mediated cyclin-CDK pathway and cell cycle regulation in HNSCC. Briefly, CCT2 deficiency causes lower level of right folded E3 ligases like Cdc20 and

thus enhances stability of many proteins which may include CDK4, p27, and GSK3- $\alpha/\beta$ . The enhanced p27 and GSK3- $\alpha/\beta$  inhibits the activity of cyclin-CDK complex and downstream transcription. CCT2 folds and interacts with actin, tubulins and Cdc20 to help the transition of M phase to G1 phase.

## Supplementary Files

This is a list of supplementary files associated with this preprint. Click to download.

- [SuppFigures.tif](#)
- [supplementarytable2.docx](#)
- [supplementarytable1.docx](#)